JCI The Journal of Clinical Investigation

Peptide vaccination of mice immune to LCMV or vaccinia virus causes serious CD8$^+$ T cell-mediated, TNF-dependent immunopathology

Fei Liu, … , Daniel E. Hassett, J. Lindsay Whitton

J Clin Invest. 2006;116(2):465-475. https://doi.org/10.1172/JCI25608.

Research Article Virology

CD8$^+$ T cells play a key role in clearing primary virus infections and in protecting against subsequent challenge. The potent antiviral effects of these cells make them important components of vaccine-induced immunity and, because of this, peptide vaccines often contain epitopes designed to induce strong CD8$^+$ T cell responses. However, the same effector functions that protect the host also can be harmful if they are not tightly regulated, and virus-specific CD8$^+$ T cells are a frequent cause of immunopathology. Here, we report that the administration of peptide to virus-immune recipient mice can lead to the synchronous activation of preexisting virus-specific CD8$^+$ T cells with serious, and even lethal, consequences. Mice infected with LCMV or vaccinia virus developed rapid and profound hypothermia following injection of cognate synthetic peptides, and LCMV-infected mice frequently died within hours. Detailed analyses of the LCMV infected mice revealed enterocyte apoptosis and implicated TNF produced by peptide-specific CD8$^+$ T cells as the major mediator of disease. The caspase inhibitor zVADfmk had no demonstrable effect on the development of hypothermia, but diminished enterocyte apoptosis and greatly reduced the number of deaths. These findings, if similarly observed in patients, counsel caution when administering powerful immunogens such as peptide vaccines to individuals who may have a large preexisting pool of epitope-specific CD8$^+$ T cells.

Peptide vaccination of mice immune to LCMV or vaccinia virus causes serious CD8+ T cell–mediated, TNF-dependent immunopathology

Fei Liu, Ralph Feuer, Daniel E. Hassett, and J. Lindsay Whitton

Department of Neuropharmacology, The Scripps Research Institute, La Jolla, California, USA.

CD8+ T cells play a key role in clearing primary virus infections and in protecting against subsequent challenge. The potent antiviral effects of these cells make them important components of vaccine-induced immunity and, because of this, peptide vaccines often contain epitopes designed to induce strong CD8+ T cell responses. However, the same effector functions that protect the host also can be harmful if they are not tightly regulated, and virus-specific CD8+ T cells are a frequent cause of immunopathology. Here, we report that the administration of peptide to virus-immune recipient mice can lead to the synchronous activation of preexisting virus-specific CD8+ T cells with serious, and even lethal, consequences. Mice infected with LCMV or vaccinia virus developed rapid and profound hypothermia following injection of cognate synthetic peptides, and LCMV-infected mice frequently died within hours. Detailed analyses of the LCMV infected mice revealed enterocyte apoptosis and implicated TNF produced by peptide-specific CD8+ T cells as the major mediator of disease. The caspase inhibitor zVADfmk had no demonstrable effect on the development of hypothermia, but diminished enterocyte apoptosis and greatly reduced the number of deaths. These findings, if similarly observed in patients, counsel caution when administering powerful immunogens such as peptide vaccines to individuals who may have a large preexisting pool of epitope-specific CD8+ T cells.

Introduction

CD8+ T cells play an important role in combating many primary virus infections, and their memory cell progeny contribute to protection against subsequent encounters with the same agent (1). The antiviral effects of these cells are mediated either by lysis of the infected target cell (2, 3), or by the secretion of potentially toxic cytokines such as IFN-γ and TNF (4, 5). These effects are often cytopathic, and, consequently, antiviral T cell responses usually are accompanied by some degree of immunopathology. Indeed, the systemic symptoms of many virus infections (headache, muscle aches, fever or chills) result not from the infection itself, but from the immune response thereto. The simultaneous activation of many host T cells can have potentially catastrophic consequences, as demonstrated in animal models by the administration of a superantigen (SAg) such as staphylococcal enterotoxin B. SAgs are bacterial or viral gene products that interact with MHC class II molecules, causing polyclonal activation of T cell receptors on CD4+ (and sometimes CD8+) T cells; some SAgs can stimulate up to 20% of all naive T cells, and this broad stimulatory capacity can cause dramatic immunopathological effects, sometimes culminating in lethal shock (reviewed in ref. 6). The iatrogenic initiation of SAg-induced shock is improbable, because compounds known to trigger SAg activity are unlikely to be intentionally administered to humans at a high dose. In contrast, synthetic peptides are considered promising candidates for new-generation vaccines and, in such a role, would be delivered to many millions of people worldwide. Peptide vaccination is attractive for a number of reasons. Peptides are chemically well-defined and can be obtained in abundance. Furthermore, epitope mapping of high-risk infectious agents is a major focus of the NIH biodefense program; this ensures that the epitope database — which already contains many microbial and tumor sequences — will grow dramatically in the coming years. Peptides are poorly immunogenic by themselves but, when delivered with adjuvant, can be quite effective; the combined results of many clinical trials of peptide vaccination against tumors — mainly malignant melanoma — indicate that a majority of peptide-vaccinated individuals generate a detectable immune response, and some 10–20% derive clinical benefit (reviewed in ref. 7).

At first blush, it appears unlikely that the administration of synthetic peptides holds, for the recipient mouse, any risk analogous to SAg stimulation, because the stimulatory capacity of an epitope peptide is very limited in the naive host. A peptide will activate only those naive precursor cells that express the appropriate epitope-specific TCR; and it has been suggested that the precursor frequency of naive T cells specific for any given epitope peptide is approximately 1 in 10^5 (~100 cells per mouse spleen) (8). However, virus infections often lead to the explosive expansion of epitope-specific T cells. For example, studies of lymphocytic choriomeningitis virus (LCMV) infection in mice have shown that a population of approximately 10^2 naive precursors, specific for a single viral epitope, can expand to approximately 10^7 cells within a 7- to 8-day period and can come to represent more than 50% of all CD8+ T cells in the infected host. Furthermore, even after the infection has been cleared, and the acute response has subsided, some 5×10^5 epitope-specific cells may remain, representing approximately 5–10% of the total CD8+ T cell population. Such dramatic expansion of virus-specific primary CD8+ T cells, and the retention of large numbers of memory cells, are not limited to this animal model; humans,

Nonstandard abbreviations used: ICCS, intracellular cytokine staining; LCMV, lymphocytic choriomeningitis virus; mTNF, membrane-bound TNF; POA, preoptic area; RPA, RNase protection analysis; SAg, superantigen; sTNF, soluble TNF; TNFR, TNF receptor.

Conflict of interest: The authors have declared that no conflict of interest exists.

Citation for this article: *J. Clin. Invest.* **116**:465–475 (2006). doi:10.1172/JCI25608.

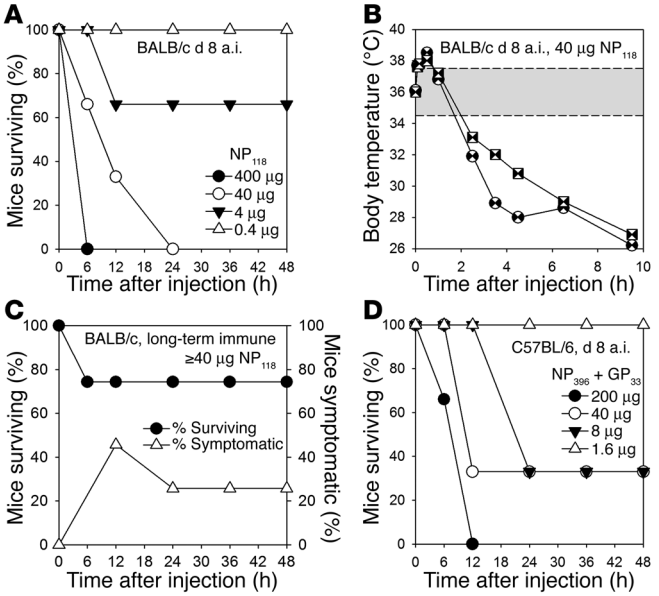

Figure 1
Peptide inoculation can cause lethal shock in infected or immune vaccinees. (**A**) BALB/c mice (3 mice per group) were infected with LCMV and, 8 days later, were inoculated i.v. with the indicated amounts of NP_{118} peptide, and their survival was determined over a 48-hour period. (**B**) Two BALB/c mice were implanted with IPTT-100 temperature probes 2 days before they were infected with LCMV. Eight days after infection (a.i.), each mouse was injected i.v. with 40 μg of NP118, and their body temperatures were monitored over the course of 10 hours. (**C**) Long-term immune BALB/c mice (a total of 35 mice, in 9 experiments) received NP_{118} peptide and were observed for survival (circles) and for the development of clinical signs (described in the text; triangles). (**D**) An experiment similar to that described in **A** was carried out, this time using C57BL/6 mice, and a mixture of the NP_{396} and GP_{33} codominant epitope peptides as described in Methods.

too, mount strong $CD8^+$ T cell responses. For example, during a primary EBV infection, as many as 44% of all $CD8^+$ T cells in the PBMC population were specific for a single viral epitope, and more than 3 years later, 18% of $CD8^+$ T cells among the patient's PBMCs remained epitope-specific (9).

Therefore, the inoculation of a peptide representing a viral epitope might be innocuous in a naive individual but may have pathological consequences in an individual who was concurrently infected with the virus, or who had — perhaps unknowingly — been previously exposed to the microbe. Here, using 2 mouse models of virus infection, we show that injection of an epitope peptide under such circumstances can, indeed, cause symptoms that vary from mild to lethal. In addition, we identify TNF as the key effector molecule responsible for the immunopathology and demonstrate that some, but not all, of the symptoms can be abrogated by the administration of a caspase inhibitor. Thus, peptide immunization should be used with some caution, if there is a risk that the vaccinee may have an existing pool of activated, epitope-specific primary or memory $CD8^+$ T cells.

Results

Peptide immunization of acutely infected mice causes lethal shock. These studies were initiated not to evaluate the risks of peptide immunization, but instead to determine how $CD8^+$ T cells respond to in vivo antigen contact in various organs and tissues. In a pilot experiment, BALB/c mice that had been infected with LCMV 8 days previously were inoculated i.v. with 40 μg of a synthetic peptide representing the LCMV epitope NP_{118} (RPQASGVYM, presented by the L^d MHC class I allele), or with saline alone. The saline control mice displayed no clinical signs. In contrast, all of the peptide-injected mice (4 of 4) died within 24 hours of injection. Before death, these mice developed several shocklike signs, the severity of which increased over time. These included hunched backs, apparent hypothermia (the mice became cool to the touch), reduced mobility, unresponsiveness, tremor, and eventually death. Thus, our observations that the administration of peptide antigen to an immune host could cause very substantial harm were serendipitous, but, because peptide vaccines have been proposed for human use and have been evaluated in clinical trials, we considered it important to characterize the risks that might be associated with this mode of immunization, and to identify the pathological mechanism(s) underlying the resulting disease.

First, we determined whether the peptide-induced pathology was dose-dependent. BALB/c mice were infected with LCMV and, 8 days later, received a single inoculation of NP_{118} peptide. Four groups of mice received peptide doses that varied over a 1,000-fold range. As shown in Figure 1A, all infected mice that received 400 μg or 40 μg died within 24 hours, with death being more rapid in the higher-dose group. Only a proportion of mice that received 4 μg peptide succumbed, and none of the mice that received 0.4 μg died. To quantitate our clinical observation of hypothermia, microchip temperature transponders were implanted s.c. into 2 BALB/c mice; the gray box in Figure 1B shows the normal range of temperatures in infected mice measured using this microchip. The mice were infected with LCMV and, at 8 days postinfection, were injected with 40 μg NP_{118} peptide. As shown, a brief elevation in temperature was observed immediately after injection, perhaps due to the heat lamp exposure used to facilitate the injection procedure. Within 1–2 hours of peptide injection, the s.c. temperatures of both mice began to fall sharply, and this precipitous decline continued; 10 hours after peptide administration, both

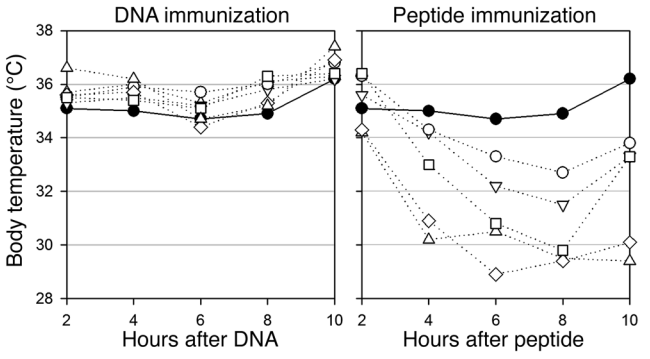

Figure 2
Clinical signs are induced by intramuscular immunization with peptide, but not with DNA. At 8 days after LCMV infection, microchip-implanted C57BL/6 mice received saline alone (filled circles, solid lines) or a vaccine containing both the NP_{396} and the GP_{33} epitopes (open symbols, dotted lines); the vaccine was either a mixture of plasmids encoding the viral NP and GP (left panel), or the NP_{396} plus GP_{33} peptide mix (right panel). After injection, their body temperatures were determined every 2 hours.

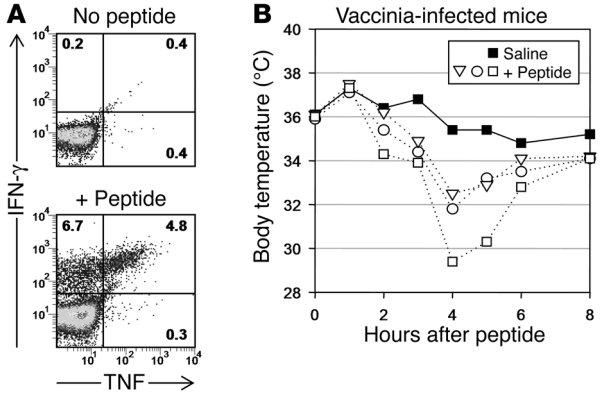

Figure 3
Vaccinia virus–infected mice mount strong CD8+ T cell responses and develop rapid and marked hypothermia following peptide inoculation. (**A**) Four C57BL/6 mice were infected with vaccinia virus and, 9 days later, were sacrificed, and their CD8+ T cell response to peptide $B8R_{20–27}$ was evaluated by ICCS. (**B**) Four C57BL/6 mice were implanted with microchips and infected with vaccinia virus. Eight days after infection, 3 mice were inoculated with $B8R_{20–27}$ peptide (open symbols, dotted lines) and 1 with saline (filled symbols, solid line), and temperatures were recorded over an 8-hour period.

mice showed an s.c. temperature of approximately 26°C, and the mice died approximately 2 hours thereafter. Thus, peptide-induced immunopathology is dose-dependent, and recipient mice show signs consistent with systemic shock.

Peptide-induced symptoms also occur in long-term immune recipient mice, and in other recipient strains. The administration of peptide vaccine to a virus-infected recipient probably would be uncommon, because (a) the majority of individuals presenting for vaccination would be uninfected, and (b) individuals showing clinical signs of illness would be considered inappropriate candidates for vaccination (although exceptions to these rules will be mentioned in the Discussion). However, many prospective vaccinees will have undergone (and recovered from) multiple viral infections and so will carry substantial numbers of CD8+ memory T cells specific for a variety of viruses — possibly including the virus against which the peptide vaccine is directed. Therefore, we next determined the outcome of peptide vaccination of a host that was already immune to the related virus. In several independent experiments, a total of 35 long-term immune BALB/c mice (so designated because they had recovered from LCMV infection at least 6 weeks previously) were inoculated with at least 40 μg of NP_{118} peptide. As shown in Figure 1C, approximately 25% of the mice died within hours of injection, and almost half of them developed clinical signs of illness (hunched posture, ruffled coat). Furthermore, histological changes consistent with immunopathology were observed in these survivors (see below). Therefore, peptide-induced symptoms are not limited to virus-infected recipient mice; they occur also in healthy mice that, as a result of a prior infection, are already immune to the peptide contained in the vaccine. The reduced toxicity observed in long-term immune peptide recipient mice, compared with acutely infected mice, may be related to the approximately 10-fold reduction in virus-specific CD8+ T cells present at the later time point. These toxic effects of peptide inoculation during acute infection are not unique to BALB/c mice. A dose-response experiment also was carried out in LCMV-infected C57BL/6 mice, by inoculation of various doses of a 1:1 mixture of the 2 peptides (GP_{33} and NP_{396}) that represent the dominant epitopes on the H-2^b MHC background (Figure 1D). The outcome was similar to that observed in BALB/c mice; recipients of the highest quantity of peptide all died within 12 hours, and lower doses resulted in reduced mortality.

Immunization-induced clinical signs follow peptide vaccination, but not DNA vaccination. To determine whether the profound immunopathology was specific for peptide vaccines, we evaluated another mode of immunization in infected mice. We chose to evaluate nucleic acid vaccination, which also is in clinical trials. LCMV-infected microchip-implanted C57BL/6 mice were immunized intramuscularly with a mixture of plasmids pCMV-NP and pCMV-GP, DNA vaccines that encode, respectively, the viral nucleoprotein and glycoprotein and that have been shown to induce strongly protective antiviral immunity (10, 11). A second group of mice received intramuscular injections of the NP_{396} plus GP_{33} peptide mix; and a negative control mouse was inoculated with saline alone. The mice that received DNA were clinically normal and, as shown in Figure 2, showed no reduction of body temperature; in contrast, peptide-inoculated mice suffered rapid-onset hypothermia, although they did not die, perhaps because peptide distribution was slower than when delivered i.v.

Mice acutely infected with vaccinia virus show rapid hypothermia following epitope peptide injection. The LCMV model sometimes is viewed with circumspection, because it is argued that the CD8+ T cell response mounted by virus-infected mice is not representative of other infections, especially in humans. This point is debatable; for example, it has been reported that, in a human infected with EBV, as many as 44% of all circulating CD8+ T cells are specific for a single virus epitope (9). Nevertheless, we wished to demonstrate that the acute pathology observed following injection of peptide was not restricted to the LCMV system. To this end, we chose to evaluate the outcome of peptide immunization in mice that

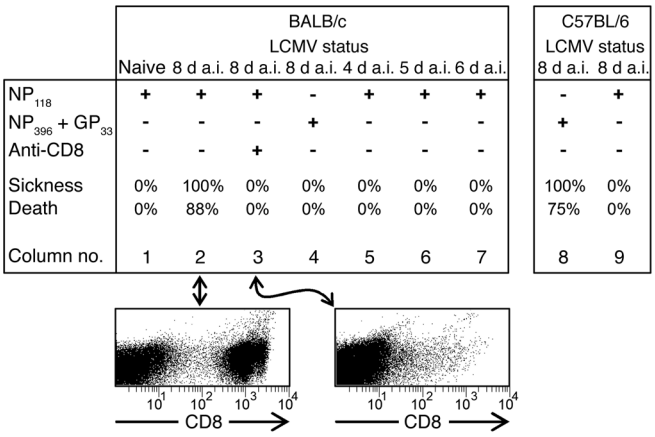

Figure 4
Morbidity and mortality following peptide vaccination require CD8+ T cells. BALB/c or C57BL/6 mice (at least 8 mice per group) received the indicated peptides at the doses described in the text. The infection status of the mice (naive or at various days after infection) is shown. A flow cytometry dot plot demonstrates the robust CD8+ T cell response at 8 days postinfection (column 2). One group of mice (column 3) received anti-CD8 antibody, and the successful depletion of CD8+ cells is shown in the related dot plot. All mice were monitored for survival, and for the development of clinical signs.

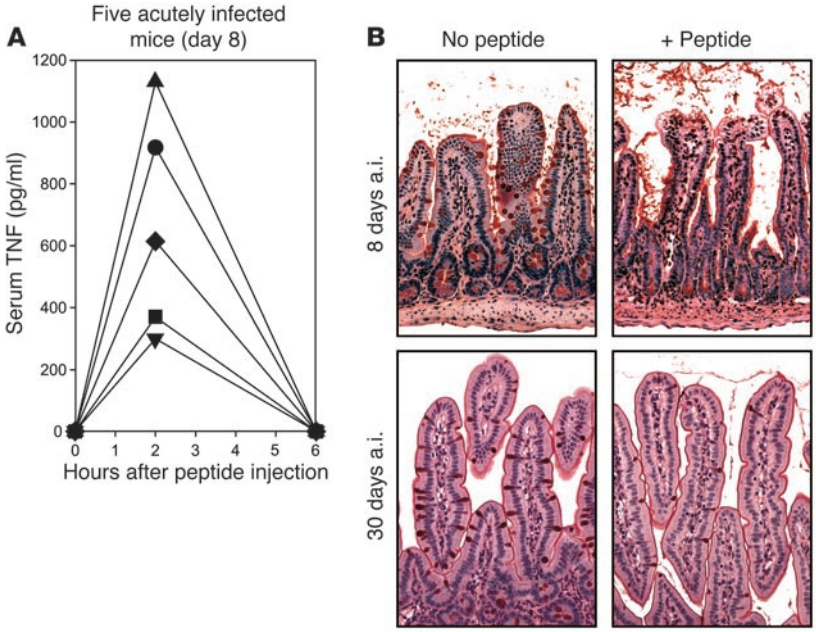

Figure 5
Peptide-induced changes implicate TNF in pathogenesis. Five C57BL/6 mice were infected with LCMV 8 days before they were injected with NP/GP peptide mix, or saline. (**A**) Blood was drawn before peptide injection and at 2 and 6 hours after injection, and serum levels of TNF were measured by ELISA. No TNF was detected in saline-injected mice (data not shown). (**B**) Twelve hours after saline injection (left column) or NP/GP peptide injection (right column) of acutely infected mice (top row) or of long-term immune mice (bottom row), histological sections of the jejunum were obtained and stained with PAS and hematoxylin. Red-staining mucinogen was detected in goblet cells, and expelled mucin was detected in the intestinal lumen. Magnification, ×20.

were acutely infected with vaccinia virus. This model was selected for 3 reasons. First, the vast majority of adult humans have been immunized with this virus and will have virus-specific memory T cells (12). Second, in the event of the reappearance of smallpox, peptides may be used to "ring vaccinate" to limit infection, raising the possibility that acutely infected humans will receive a high dose of poxvirus-specific peptide. Third, murine epitopes for vaccinia virus have recently been described (13). Therefore, a group of microchip-implanted C57BL/6 mice were infected with vaccinia virus. As reported, these mice develop strong $CD8^+$ T cell responses, with approximately 11.5% of splenic $CD8^+$ T cells responding to in vitro incubation with the dominant peptide, $B8R_{20–27}$ (Figure 3A). Most relevant to the present study, the injection of 100 μg of the $B8R_{20–27}$ peptide 8 days after vaccinia infection resulted in a very rapid hypothermia (Figure 3B), although all mice recovered.

The pathological effects of peptide injection require virus-specific $CD8^+$ T cells. A role for $CD8^+$ T cells in disease pathogenesis was indicated by the finding that virus-infected and long-term virus-immune mice developed severe pathological signs after receiving a peptide representing a viral $CD8^+$ T cell epitope. The requirement for $CD8^+$ T cells was confirmed and characterized in several ways (Figure 4). Injection of the NP_{118} peptide into naive mice caused no morbidity (column 1), indicating the importance of prior virus infection in the lethal disease (column 2; the high number of $CD8^+$ T cells in these mice at 8 days postinfection is shown by flow cytometry). One group of virus-infected mice was depleted of $CD8^+$ T cells before peptide injection (column 3; approximately 95% of $CD8^+$ T cells were depleted, as indicated by the flow cytometry dot plot); these mice survived NP_{118} injection and showed no signs of illness. The requirement for epitope-specific $CD8^+$ T cells in pathogenesis was confirmed by the absence of toxicity of the NP_{396} plus GP_{33} peptides in day 8 BALB/c mice (column 4), a finding that was borne out by the reciprocal experiment, in which day 8 C57BL/6 mice developed severe disease after injection with the $H\text{-}2^b$ peptides NP_{396} plus GP_{33} but were undisturbed by inoculation of the major $H\text{-}2^d$ epitope peptide NP_{118} (columns 8 and 9). These data demonstrate unequivocally that, in both BALB/c and C57BL/6 mice, peptide-specific $CD8^+$ T cells are required for both the morbidity and the mortality that result from peptide inoculation. In addition, we found that clinical disease required that the $CD8^+$ T cell response be at a relatively advanced stage: peptide injection of mice at 4–6 days postinfection induced no signs of sickness (columns 5–7). This may be attributable to the lower

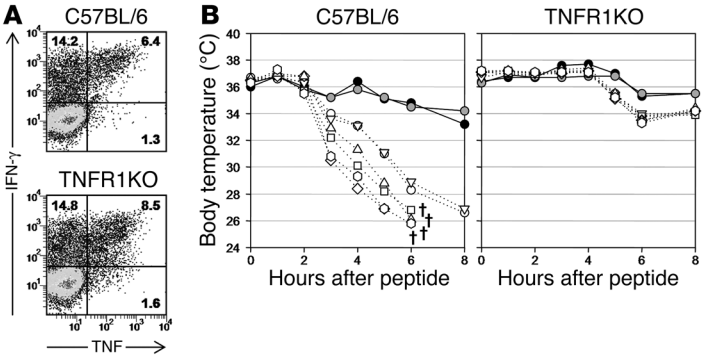

Figure 6
Clinical effects of peptide injection do not occur in mice lacking TNFR1. (**A**) C57BL/6 or TNFR1KO mice (4 per group) were infected with LCMV and, 8 days later, were sacrificed, and their virus-specific $CD8^+$ T cell responses were measured by ICCS, as described in Methods. Dot plots are gated on $CD8^+$ T cells; the *y* axis shows IFN-γ staining, and the *x* axis shows TNF staining. Numbers in each of 3 quadrants indicate the $CD8^+$ T cells in that quadrant as a percentage of total $CD8^+$ T cells. (**B**) C57BL/6 or TNFR1KO mice (8 per group) were microchip-implanted, and infected with LCMV. Eight days later, the mice were injected either with peptide (6 mice per group, open symbols, dotted lines) or with saline (2 mice per group, filled symbols, solid lines), and their body temperatures were measured over the subsequent 8 hours. Crosses indicate deaths that occurred before the end of this period.

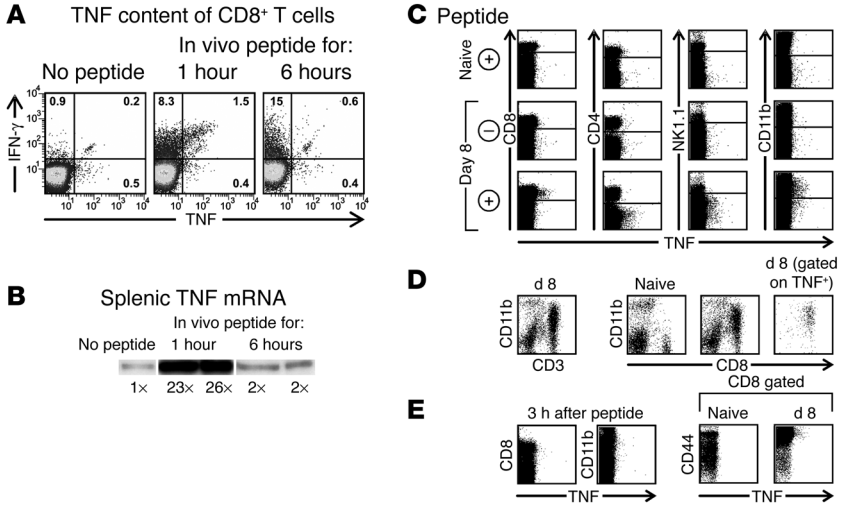

Figure 7

TNF production, and consequent immunopathology, are largely attributable to CD8+ T cells. (**A** and **B**) Five C57BL/6 mice were infected with LCMV and, 8 days later, 4 received NP/GP peptide mix. One hour later, 2 peptide-inoculated mice were sacrificed, and the remaining 3 were sacrificed after a further 5 hours. Immediately after sacrifice, spleens were processed for direct ICCS and RPA. (**A**) TNF content of live CD8+ T cells is shown in mice that received no peptide and in mice at 1 and 6 hours after peptide inoculation. (**B**) The band intensities for TNF mRNA were measured using NIH ImageJ. The "no peptide" sample was assigned a value of 1; fold increases in signal in the other samples are shown below each lane. (**C**–**E**) Seven mice were infected with LCMV, and, 8 days later, 2 were inoculated with saline and the remaining 5 received NP/GP peptide mix, which was also administered to 2 naive mice. One hour later, 5 mice (3 infected/peptide, 1 infected/saline, and 1 naive/peptide) were sacrificed, and the remaining mice (2 infected/peptide, 1 infected/saline, and 1 naive/peptide) were sacrificed after a further 2 hours. Immediately after sacrifice, spleens were analyzed using direct ICCS (no peptide incubation). (**C**) TNF production at 1 hour after peptide injection. (**D**) Only $CD11b^{hi}CD8^+$ T cells produce TNF at 1 hour after peptide injection. (**E**) Left: $CD11b^{hi}$ cells and $CD8^+$ cells had terminated TNF production by 3 hours after peptide injection. Right: Only $CD44^{hi}$ cells produced TNF at 1 hour after peptide injection (gated on $CD8^+$ cells).

numbers of virus-specific CD8+ T cells present at earlier times, but we consider this unlikely, because the cell numbers at 6 days after infection exceeded those present in long-term immune mice, which developed signs following peptide injection (Figure 1C). The key factor may be not the quantity of virus-specific CD8+ T cells, but rather their quality. We have previously shown that, over the course of virus infection, virus-specific CD8+ T cells undergo several types of functional maturation that result in their becoming better able to mount effective antiviral responses (14–16). These maturation processes have been most fully characterized for IFN-γ but occur also for TNF (15) and continue until at least 8 days after infection, after which time the cells, and their memory cell progeny, retain this high responsiveness. We speculate that the absence of peptide-mediated effects in mice at 4–6 days after infection may reflect the relatively immature functional status of the virus-specific cells; by day 8, and in the memory phase, the cells are more readily triggered by antigen contact.

TNF is implicated in peptide-driven immunopathology. The rapidity and characteristics of the peptide-induced symptoms, including the dramatic hypothermia, are reminiscent of septic shock, in which a key role is played by bacterially induced host cytokines such as TNF and IL-6 (17). Macrophages serve as the major source of TNF in septic shock, but this cytokine also is rapidly produced by CD8+ T cells following antigen contact, and, therefore, TNF was an obvious suspect in the peptide-mediated CD8+ T cell–dependent disease and death. To investigate this issue, 5 day 8 LCMV-infected C57BL/6 mice were injected with 200 μg of NP_{396} plus GP_{33} peptides, and blood was drawn from each mouse, immediately prior to peptide injection (time 0) and at 2 and 6 hours after injection. As shown in Figure 5A, all 5 mice had high quantities of TNF in their sera at 2 hours after injection, but the levels had fallen to background as early as 4 hours later. A very similar pattern of rapid ascent of serum TNF, to levels as high as approximately 1,000 pg/ml, followed by equally rapid descent, has been previously described in mouse models of LPS-induced shock (18, 19). Next, we determined whether or not the mice showed physical signs of TNF toxicity. Mice were infected with LCMV, and, 8 days later, some were inoculated with the mixture of NP and GP peptides; all mice were sacrificed 8 hours later. In at least 3 separate experiments, mice that had received the peptide mix showed visible dilation of the small intestines, which were filled with yellow, viscous fluid. These observations are consistent with acute TNF toxicity (20, 21), in which intestinal changes can occur with extraordinary speed, being detectable within 30 minutes of injection of recombinant TNF (22). Histological sections of the small intestines from acutely infected mice, without and with peptide injection (200 μg NP_{396} plus GP_{33} peptide mix), are shown in the top row of Figure 5B. The sections were stained using PAS, which renders complex carbohydrates a deep red color, and were counterstained with hematoxylin. In the absence of peptide injection (Figure 5B, left panels), no intestinal pathology was visible; numerous mucinogen-containing goblet cells are identified by the PAS stain. In contrast, 6 hours after peptide injection of acutely infected mice, 3 striking histological changes were visible. First, the intestinal lumen contained abundant mucin, reflecting the very rapid release of mucinogen, and its subsequent explosive swelling (several-hundred-fold in a few seconds; ref. 23). Second, the goblet cells were less readily identified, because they had expelled their mucinogen contents. Third, the tops of the villi were blunted, in what has been termed the "lawnmower effect." All 3 pathological signs have been associated with acute TNF toxicity (20–22). An equivalent analysis was carried out in LCMV-immune mice (day 30 after infection), which also developed symptoms following peptide inoculation (Figure 1C), albeit to a lesser degree than acutely infected mice. Pathological changes were detectable (Figure 5B, bottom row): compared with sham-inoculated immune mice, peptide-inoculated immune mice had fewer PAS+ goblet cells, and a correspondingly greater amount of mucin in the intestinal lumen. However, no villus blunting was observed. Thus, the extent of histopathology following antigen exposure of acutely infected or immune mice is consistent with their differing clinical outcomes. In contrast to

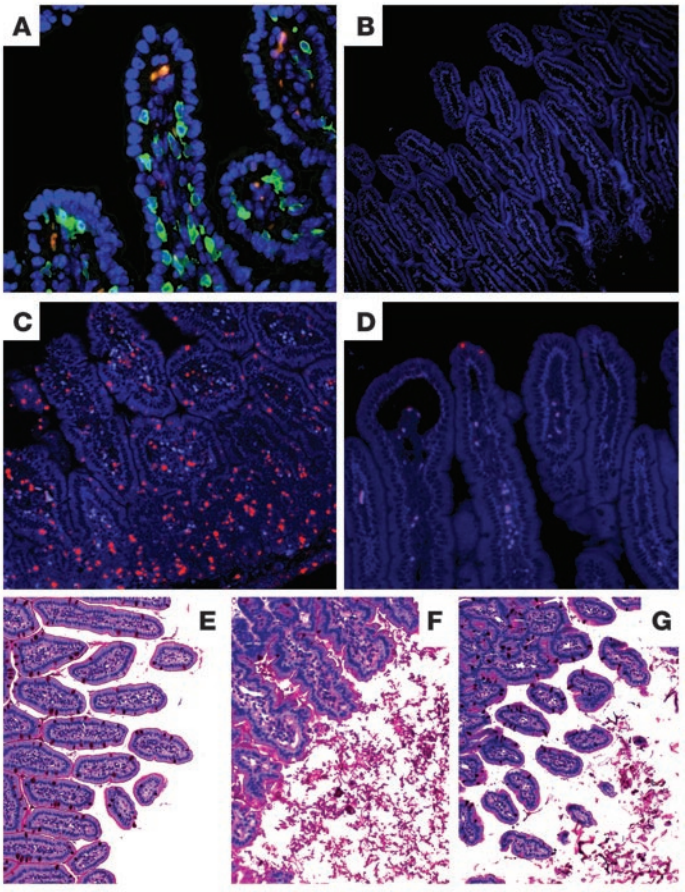

Figure 8
zVADfmk blocks peptide-induced intestinal apoptosis, but not mucin exocytosis. C57BL/6 mice at 8 days postinfection were injected with either peptide or saline. Some mice from each group were treated with zVADfmk, as described in the text. (**A**–**D**) DAPI staining (blue) was used to identify cell nuclei; **B**–**D** are overexposed to allow the villus outlines to be visualized. (**A**) Anti-CD3 staining (green) reveals T cells in the intestinal villi. **B**–**D** were stained using the ApopTag kit; apoptotic cells contain red nuclei. Mice had received (**B**) saline, (**C**) peptide, or (**D**) peptide and zVADfmk. (**E**–**G**) PAS-stained jejunums from mice that had received (**E**) saline, (**F**) peptide, or (**G**) peptide plus zVADfmk. Magnification, ×40 (**A**), ×20 (**B**–**G**).

the rapid appearance of histological changes in the intestine, neither macroscopic nor histopathological changes were observed in the spleens, lungs, kidneys, or livers of these mice, when evaluated 8 hours after peptide injection.

Clinical signs of peptide injection do not occur in mice lacking TNF receptor 1. Two receptors for TNF have been identified: TNFR1 is a 55-kDa protein that is constitutively expressed in most tissues, and TNFR2 is a 75-kDa molecule with tightly regulated expression that is found most often on cells of the immune system. Current understanding suggests that the majority of systemic TNF-mediated effects occur via TNFR1 signaling (24), and TNFR1 is thought to mediate antiviral activity (25). For these reasons, we chose to evaluate the effects of peptide injection in mice lacking this protein (TNFR1KO mice). These mice mount strong $CD8^+$ T cell responses to LCMV Armstrong infection and eradicate the virus with kinetics similar to those observed in normal mice (26), so these studies were not compromised by the reduced T cell numbers and/or viral persistence that occurs following LCMV infection of several other knockout mouse lines (e.g., perforin knockout [ref. 2] and IFN-γ knockout [refs. 27, 28] strains). TNFR1KO and C57BL/6 mice were infected with LCMV, and, 8 days later, their virus-specific $CD8^+$ T cell responses were evaluated by intracellular cytokine staining (ICCS). As shown in Figure 6A, both strains of mice mounted $CD8^+$ T cell responses, confirming the recent, more detailed, analyses from another laboratory (26). Next, microchip-implanted TNFR1KO and C57BL/6 mice (8 mice per group) were infected with LCMV, and, 8 days later, 6 mice in each group were inoculated with the NP/GP peptide mix, and their temperatures were measured at the indicated times (Figure 6B). Within 2–3 hours of peptide injection, the body temperatures of C57BL/6 mice began to fall, and 4 of the 6 mice died approximately 7 hours after injection. In contrast, all of the peptide-injected TNFR1KO mice survived and showed only a very minor reduction in temperature, following the diurnal pattern evident in their noninjected counterparts. In a subsequent experiment, 2 TNFR1KO mice were sacrificed 6 hours after peptide injection; no macroscopic changes in the gut were visible, and histological analyses showed minimal mucin in the lumen, normal numbers of goblet cells, and no villus blunting (data not shown). Therefore, TNFR1 is required for the temperature reduction, mucin exocytosis, and lethal outcome that can result from peptide injection.

Pathological outcome is likely to be attributable to TNF produced by virus-specific $CD8^+$ T cells. The foregoing data prove that (a) peptide-driven activation of $CD8^+$ T cells is required for pathology (Figure 4); (b) serum TNF increases rapidly after peptide injection (Figure 5A); (c) the histological changes are consistent with TNF-mediated events (Figure 5B); (d) $CD8^+$ T cells synthesize TNF following peptide injection (Figure 6A); and (e) pathology is TNF-dependent (Figure 6B). Taken together, these data suggest that the pathological consequences of peptide injection are mediated by TNF that is released from $CD8^+$ T cells. However, it remains possible that the effect is indirect; perhaps the peptide-activated $CD8^+$ T cells activate other cell types, causing them to elaborate TNF, thereby contributing to the clinical outcome. We investigated this question in 2 ways. First (Figure 7, A and B), we evaluated the kinetics of TNF production by $CD8^+$ T cells. Mice infected 8 days previ-

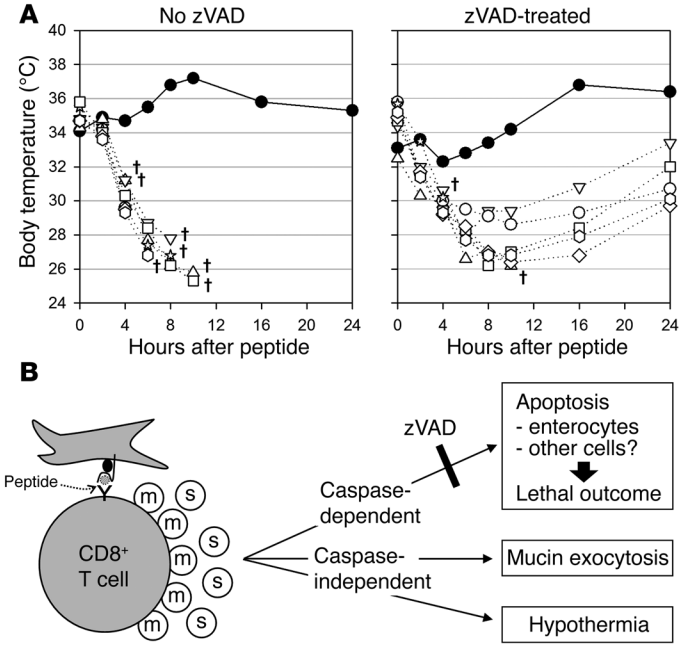

Figure 9
zVADfmk has no effect on hypothermia but protects against lethal outcome. (**A**) Sixteen C57BL/6 mice were implanted with IPTT-100 temperature probes 2 days before they were infected with LCMV. Eight days after infection, 8 mice were injected with 1 mg of zVAD-fmk. An hour later, 7 mice from each group were injected with peptide, while 1 mouse was injected with saline, and body temperatures were monitored over the next 24 hours. (**B**) A diagrammatic summary of the effects of peptide injection of virus-immune mice. The cell at the top left represents any MHC class I$^+$ somatic cell. m, membrane TNF; s, soluble TNF.

ously with LCMV were inoculated with the NP/GP peptide mix and were sacrificed at 1 hour or 6 hours after injection. Sections of the spleens were immediately processed for evaluation of TNF and IFN-γ content (without in vitro incubation with peptide) and for RNA purification, and subsequent RNase protection analysis (RPA). As shown in Figure 7A, LCMV-infected mice harbored few cytokine-positive cells at 8 days after infection, consistent with the low levels of endogenous antigen at this time point. Within 1 hour of peptide injection, a substantial population of CD8$^+$ T cells had begun to elaborate abundant TNF, and, by 6 hours after peptide injection, these cells had terminated TNF production, although they continued to make IFN-γ. This on/off regulation of TNF following antigen contact in vivo has not, to our knowledge, been previously reported but is consistent with in vitro observations by Harty and colleagues (29). Because TNF expression by virus-specific CD8$^+$ T cells in vitro is regulated largely at the transcriptional level (30), we also investigated the in vivo levels of TNF mRNA in the spleens of these mice. TNF mRNA was identified by RPA, and band intensities were quantitated using ImageJ software. As shown in Figure 7B, TNF mRNA was approximately 25-fold higher than the resting level by 1 hour after peptide injection, and, by 6 hours after injection, it had declined almost to constitutive levels. There was minimal change in the levels of mRNA for lymphotoxin-α (data not shown), the only other member of the TNF family that binds to TNFR1 (31). Thus, there is a strong relationship between peptide-driven increases in splenic TNF mRNA and TNF protein in CD8$^+$ T cells, and both measurements parallel the rapid rise and fall in serum levels reported in Figure 5A; these data are consistent with the interpretation that the high levels of serum TNF are derived directly from the peptide-stimulated CD8$^+$ T cells.

As the second approach to determining the possible role of other cells in detrimental TNF production, other likely sources of TNF were investigated. As shown in Figure 7C, the great majority of TNF-producing cells were CD8$^+$ (first column), and very few cells expressed CD4 or NK1.1. However, many TNF$^+$ cells expressed high levels of CD11b (Mac-1; Figure 7C, fourth column), raising the possibility that macrophages (which express high levels of this marker; ref. 32) had been stimulated to produce TNF. However, CD11b also is expressed by activated CD8$^+$ T cells of mice (33) and humans (34), and subsequent analyses, reported below, indicated that the TNF$^+$CD11b^{hi} cells were virus-specific CD8$^+$ T cells. A large population of CD11b^{hi} T cells (CD3$^+$ cells) was present at day 8 after infection (Figure 7D, first dot plot), and CD11b^{hi}CD8$^+$ T cells were scarce in naive mice but were abundant in day 8 mice (Figure 7D, second and third dot plots). Furthermore, when splenocytes harvested 1 hour after peptide injection were gated on TNF$^+$ cells, the great majority were both CD8$^+$ and CD11b^{hi} (Figure 7D, fourth dot plot). Finally, the population of TNF$^+$CD11b^{hi} cells disappeared by 3 hours after peptide injection, coinciding with the loss of TNF$^+$CD8$^+$ T cells (Figure 7E, first and second dot plots); and only antigen-experienced (CD44^{hi}) CD8$^+$ T cells produced TNF in response to peptide injection (Figure 7E, third and fourth dot plots). We conclude that, after peptide injection, the great majority of serum TNF is produced by virus-specific CD8$^+$ T cells.

Peptide injection induces apoptosis, which is prevented by the pan-caspase inhibitor zVADfmk. One of TNF's major functions is the induction of apoptosis (20), and others have shown that apoptotic enterocytes can be observed within 30–90 minutes of injection of recombinant TNF, and that this can be prevented by the pan-caspase inhibitor zVADfmk (22). Our observation of blunted villi and mucin exocytosis following peptide injection suggested that the endogenous production of TNF by antigen-specific CD8$^+$ T cells also might cause enterocyte apoptosis. To evaluate this possibility, and to determine the effects of caspase inhibition on these phenomena, C57BL/6 mice were infected with LCMV, and, 8 days later, the mice were divided into 4 groups. One group was injected with diluent alone and acted as a control; the second group was inoculated with the NP/GP peptide mix; the third group received only the caspase inhibitor zVADfmk; and the fourth received both zVADfmk and peptide mix. Ten hours later, some of the mice were sacrificed and their tissues evaluated by histopathology, while others were observed for survival. First, anti-CD3 antibody was

used to identify T cells within the tissue. As shown in Figure 8A, these cells (green) were abundant within the villi of mice that had received neither peptide nor zVADfmk; the cells were present also in the plicae circulares, the muscularis mucosae, and the submucosa, and there was no perceptible difference in the abundance or distribution of cells in mice in the other 3 experimental groups (data not shown). Staining for apoptotic cells in the intestine of LCMV-infected mice that had received neither peptide nor zVADfmk revealed no evidence of apoptosis (Figure 8B), but, in contrast, apoptotic cells (red) were abundant in peptide-injected mice (Figure 8C), indicating the very rapid pathological effects of peptide-driven $CD8^+$ T cell activation. The prior administration of zVADfmk largely prevented apoptosis (Figure 8D), indicating that this TNF-driven process is caspase-dependent. However, peptide-driven mucin exocytosis was not prevented by zVADfmk. Histological sections of the jejunums of LCMV-infected mice are shown in Figure 8, E–G. In the absence of peptide injection, mucinogen-filled goblet cells were abundant, the intestinal lumen contained very little mucin, and the villi appeared healthy (Figure 8E). Peptide injection resulted in villus deformation, the almost complete loss of mucinogen-filled goblet cells, and abundant luminal mucin (Figure 8F). Peptide-injected mice treated with zVAD showed a reduction in visible goblet cells, and extensive luminal mucin, but villus deformation was not observed (Figure 8G). Thus, the enteric effects of TNF toxicity may have different molecular pathways; the rapid expulsion of mucinogen from goblet cells is barely affected by zVADfmk, while enterocyte apoptosis and the consequent villus deformation can be blocked by this caspase inhibitor.

zVADfmk does not mitigate peptide-induced hypothermia but protects against peptide-mediated death. The observation that zVADfmk prevented enterocyte apoptosis led us to investigate whether this compound also might ameliorate the clinical signs of hypothermia and death. To this end, 2 groups of microchip-implanted C57BL/6 mice (8 mice per group) were infected with LCMV. Eight days later, 1 group of mice received zVADfmk; then 7 of the mice in each group were inoculated with the NP/GP peptide mix, and their temperatures were measured at the indicated times (Figure 9A). The body temperatures of all 14 peptide-injected mice fell rapidly, indicating that zVADfmk did not protect against hypothermia. Peptide-induced mortality was 100% in mice that did not receive zVADfmk, but 5 of the 7 mice that received zVADfmk survived, and their body temperatures began to ascend toward normal after approximately 10 hours after peptide injection. Combining data from 3 independent experiments, 14 of 17 zVADfmk-treated mice survived peptide injection, compared with 4 of 17 in the untreated group; the effect of zVADfmk administration on survival is highly statistically significant ($P < 0.00025$; 2-tailed Student's t test; $P < 0.05$ was considered statistically significant).

Discussion

Herein, we show that peptide immunization of a virus-immune host can activate existing epitope-specific $CD8^+$ T cells, with detrimental effects on the recipient, as summarized diagrammatically in Figure 9B. The key mediator of the peptide-induced disease is TNF, the prototype of more than 20 related cytokines that act via members of the TNFR superfamily. The 26-kDa TNF monomer is a type II transmembrane protein that is expressed on the cell membrane as a stable homotrimer. This membrane-bound TNF (mTNF) is cleaved by the metalloproteinase TNF-α–converting enzyme (35) to release the 51-kDa soluble TNF (sTNF) trimer. Although most studies of TNF activities have focused on sTNF, mTNF also is biologically active and can trigger cytolysis and apoptosis following contact with $TNFR^+$ cells (36). TNF has been strongly implicated in a number of human diseases, including septic shock, various arthritides, and certain inflammatory bowel diseases. The in vivo toxic effects of TNF are manifold, but the earliest histological changes occur in the intestine (20). TNF-dependent, $CD8^+$ T cell–dependent events have been reported in various mouse models of inflammatory bowel disease (37, 38), and TNF also has been implicated in human intestinal disease; indeed, anti-TNF antibodies have proven beneficial in the majority of patients with Crohn disease (39). Here, we show that peptide vaccination of immune mice can result in TNF-dependent intestinal pathologies including mucin exocytosis and enterocyte apoptosis, only the latter of which can be largely prevented by zVADfmk. Our data do not prove that soluble TNF — as distinct from the membrane-bound form — is responsible for the pathological consequences of peptide inoculation. However, mice that express mTNF, but not sTNF, show markedly increased resistance to LPS-induced shock (40), implicating sTNF in that shock paradigm, and this, together with the extremely high levels of sTNF observed after peptide injection (Figure 5A), leads us to view sTNF as the main suspect. The data in Figures 6 and 8 show that enterocyte apoptosis and host death are both mediated by TNF, and the experiments with zVADfmk (Figures 8 and 9) suggest that both effects are caspase-dependent, consistent with the previous reports from other laboratories (22, 41). We believe it likely that the 2 effects are related: extensive apoptosis of enterocytes (and, possibly, of other somatic cells) may be lethal. However, some of the TNF-driven toxic effects are caspase-independent, consistent with other reports of TNF-driven, caspase-independent, cellular effects (42). The various TNF-mediated effects, and their dependence on caspases, are summarized in diagrammatic form in Figure 9B.

TNF, along with IL-6 and IL-1β, is considered one of the key mediators of fever in septic shock. However, many of the experiments in which TNF was shown to have pyrogenic effects used direct injection of recombinant protein, rather than endogenous synthesis of mTNF/sTNF, and the role of TNF in thermoregulation remains controversial (43). Some studies of endogenously produced TNF indicate that it may have antipyretic effects (44), and data from a cecal ligation/puncture model of shock suggest that TNF may even be a cryogen; hypothermia occurred in WT mice, but this was markedly attenuated in TNFRKO mice (45). The rapid descent of body temperature observed in our studies might be, in part, attributable to the circulatory collapse that accompanies shock. However, the great majority of the zVAD-treated mice survived peptide injection (Figure 9A), suggesting that they had not suffered circulatory collapse, but they nevertheless developed hypothermia that was similar in rapidity and degree to that observed in untreated mice. Therefore, circulatory collapse appears to be distinct from hypothermia, and we consider it likely that endogenous TNF, produced by $CD8^+$ T cells, can have a cryogenic effect. How might TNF induce hypothermia? Mammalian thermoregulation is a complex process, but the hypothalamus, and in particular the preoptic area (POA), plays a key role (46). Cells in this region express both of the TNFRs (47), and the firing rate of thermosensitive neurons in the POA is altered by direct application of TNF (48). Thus, we propose that $CD8^+$ T cell–derived TNF exerts its cryogenic effect centrally, in the POA. There are at least 2 ways in which $CD8^+$ T cell–derived TNF in the peripheral

circulation might gain access to the thermoregulatory centers of the hypothalamus. First, sTNF appears to be "chaperoned" across the blood-brain barrier by its receptors, so the TNF-dependent hypothermia observed in this study could be driven by cytokine that had crossed the blood-brain barrier. Second, the organum vasculosum laminae terminalis (OVLT), which lies in the midline of the POA, has been implicated in thermoregulation, and neurons within the OVLT respond to TNF (49); the OVLT lacks a blood-brain barrier and could be directly accessible to sTNF or, possibly, to mTNF on virus-specific T cells.

How might TNF cause the explosive release of mucinogen from goblet cells? Mucinogen is a mixture of highly glycosylated proteins that are held in a tightly condensed matrix inside goblet cell granules. The tight packing of these polyanionic molecules within the matrix is facilitated by the presence of calcium ions, which provide a shielding effect (50); removal of the Ca^{++} ions destabilizes the condensed mucinogen, leading to the rapid exocytosis of the granule contents (51). TNF and TNFRs have been associated with intracellular calcium mobilization (52, 53), leading us to propose that the TNF produced by antigen-specific $CD8^+$ T cells triggers calcium mobilization in intestinal goblet cells; and that this, in turn, leads to the rapid expulsion of mucin, and to the histological changes shown in Figure 5B and Figure 8, F and G. Intriguingly, calcium mobilization also has been implicated in the early stages of apoptosis (54), suggesting that it may represent an early common pathway in TNF signaling.

We show also that the physico-chemical nature of the vaccine affects the outcome in immune recipient mice. A DNA vaccine encoding the relevant epitopes induced no clinical signs, while the injection of synthetic peptide epitopes was harmful (Figure 2). The outcome is determined, presumably, by each vaccine's capacity to synchronously activate preexisting T cells, and the "ready-made" nature of peptide antigens appears more likely to achieve this than DNA vaccines, which must be taken up, transcribed, and translated. A previous study using the LCMV model reported that injection of the GP_{33} peptide into long-term immune mice induced a global immunosuppression that was detected in cells harvested 5 days after the final peptide injection, and incubated in vitro for a further 5 days (55); the rapid but transient hypothermia that we observed in long-term immune mice (Figure 1C) was not reported. The reason for this difference is unknown, but there are several possible explanations. To our knowledge, temperature-sensitive microchips were not used in the prior study, so it is possible that a transient temperature reduction went unnoticed. Similarly, it is possible that the surviving mice in our study did develop immunosuppression; we have focused on the acute changes that occur within hours of injection, and we did not investigate the longer-term effects (days/weeks) of peptide injection. In addition, there are several methodological differences between the studies (peptide dose, frequency, vehicle, and route of administration, and time of administration in relation to prior infection), and one of these — or some combination thereof — may have contributed to the difference in clinical outcome. The factor(s) responsible can be determined in subsequent analyses, but it is clear that, in both cases, peptide vaccination of a virus-immune host caused pathological changes. One difference between peptide vaccination and the method used in the studies reported here is that the former is carried out using peptide mixed with adjuvant, which, it could be argued, might limit the rapid systemic distribution of peptide, thereby avoiding the synchronous activation of antigen-specific T cells. However, adjuvants can strongly activate the innate immune response (56) — including macrophages (57), a prominent source of TNF — as well as augmenting the adaptive responses. Furthermore, others have shown, in a mouse model, that vaccinating with peptide plus adjuvant can cause serious immunopathology, if peptide/adjuvant boosts are administered when $CD8^+$ T cell responses are high (58). Finally, under circumstances of prior immunity, even low-level release of peptide antigen might be detrimental; relative neutropenia and lymphopenia can be caused by a dose of TNF 1,000-fold lower than that responsible for the florid intestinal signs (59).

In conclusion, our findings may be relevant to the clinical arena. We consider it unlikely that antitumor peptide vaccines would represent a substantial population health risk, for 2 reasons. First, the number of individuals who would receive these vaccines is relatively small, and second, these tumor-bearing individuals rarely have a large number of preexisting T cells that could respond to the injection of tumor epitope peptides. However, our findings may be highly relevant to antiviral peptide vaccines. Approved and effective antiviral vaccines usually are administered to millions of people each year, and under these circumstances even relatively rare side effects assume greater import. Furthermore, preexisting immunity to viruses is common, and individuals can harbor large numbers of epitope-specific memory T cells that could be synchronously triggered by peptide injection. In addition, if peptide vaccines were used to try to contain an outbreak of virus infection — for example, in the "ring vaccination" approach that was used to help eradicate smallpox, and which has been proposed to combat bioterrorist release of dangerous pathogens such as smallpox — then it is likely that a substantial number of peptide recipients would be acutely infected at the time of vaccination and would be at risk of developing peptide-driven immunopathology. We show here that mice acutely infected with vaccinia virus develop a rapid hypothermia following injection of a single poxvirus epitope peptide (Figure 3). Therefore, while we do not intend to cast a pall over an extremely promising technology, these observations counsel caution in the design, development, and administration of vaccines that have the potential to synchronously activate preexisting antigen-specific T cells.

Methods

Mice and virus. BALB/c ($H\text{-}2^d$) and C57BL/6 ($H\text{-}2^b$) mice (6–8 weeks old) were bred at the Scripps Research Institute breeding facility. Mice deficient in TNFR1 (referred to herein as TNFR1KO mice) were purchased from Jackson Laboratory; the strain designation is B6.129-Tnfrsf1atm1Mak/J. Mice were infected i.p. with 2×10^5 PFUs of lymphocytic choriomeningitis virus, Armstrong strain (LCMV). Vaccinia virus (strain WR) was grown in BSC40 cells and titered in HeLa cells, and mice were infected with 2×10^6 PFUs i.p. All experiments involving mice were preapproved by the Animal Care and Use Committee of the Scripps Research Institute.

Synthetic peptides, plasmid DNA injections, and chemicals. Peptides were purchased from Alpha Diagnostic International Inc. and were purified to 98% homogeneity by HPLC. The LCMV peptides used were NP_{118} (RPQASGVYM), GP_{33} (KAVYNFATC), and NP_{396} (FQPQNGQFI). NP_{118} was dissolved in water to make 10 mg/ml stock. NP_{396} and GP_{33} were first dissolved in DMSO and then diluted with PBS to make 10 mg/ml stock in 30% DMSO. Also used was a vaccinia epitope peptide, $B8R_{20\text{–}27}$ (TSYKFESV), which is the dominant epitope in C57BL/6 mice (13). This peptide was first dissolved in DMSO, then diluted to a stock concentration of 10 mg peptide per milliliter 70% PBS/30% DMSO. Peptides

were injected at various doses and by various routes; unless otherwise indicated in the text, 200 μg of a mixture of the NP_{396} and GP_{33} peptides was injected i.v. in 500 μl saline. Plasmid DNAs (100 μg of each plasmid) were injected bilaterally into the anterior tibial muscles. zVADfmk was purchased from MP Biomedicals and dissolved in 30% DMSO to a final concentration of 5 mg/ml, and each zVADfmk-treated mouse received a single i.v. injection of 200 μl of the stock solution (1 mg zVADfmk) 1 hour before the peptide injection.

Monitoring body temperature of mice. Implantable programmable temperature transponder microchips (IPTT-100 microchips; Bio Medic Data Systems Inc.) allow body temperature to be measured using a wireless "wand"; the reported temperatures are very similar regardless of whether implantation is s.c. or i.p. (60). In this study, the microchips were implanted s.c. in the interscapular region, and body temperatures were recorded using the wireless scanner DAS-5007 (Bio Medic Data Systems Inc.).

Depletion of $CD8^+$ T cells. Two days before peptide injection (6 days after infection), mice were inoculated i.v. with 250 μl saline containing 0.25 mg of a rat antibody against mouse CD8 (clone YTS 169.4.2). Control mice received saline alone. The effectiveness of depletion was evaluated 2 days later (the same day as peptide injection) by flow cytometry.

ICCS and ELISA. Splenocytes were harvested, and 2×10^6 cells per well were plated in 96-well plates and were incubated with 10^{-6} M synthetic peptides (described above) for 6 hours at 37°C in the presence of 5 mg/ml brefeldin A. Thereafter, the cells were stained with 0.25 μg/ml rat anti–mouse CD8a (Ly-2) antibody (CALTAG Laboratories) overnight at 4°C. Staining for other surface molecules was carried out for 30 minutes on ice. Antibodies against CD4, CD44, CD3, and CD11b were purchased from eBioscience, and against NK1.1 from BD Biosciences. All antibodies were used at a 1:100 dilution. After washing, cells were fixed in 2% formaldehyde in 1× PBS for 5 minutes, then permeabilized in 0.1% saponin with 0.1% sodium azide, 1% FBS in PBS (PermWash). Also, please give the (complete) name of the manufacturer.) Cells were then stained with 0.5 μg/ml rat anti–mouse IFN-γ antibody (XMG1.2; CALTAG Laboratories) for 30 minutes at 4°C, with or without 1 μg/ml rat anti–mouse TNF antibody (MP6-XT22; CALTAG Laboratories). Cells were thoroughly washed first with PermWash, then with 5% FBS-PBS, before being acquired on a FACScan flow cytometer (BD Biosciences). Analysis was done using CellQuest software (BD). ELISA for TNF was performed using the Ready-SET-Go! mouse TNF-α ELISA kit (model 88-7324) from eBioscience.

Histological evaluation. The spleen, lung, kidney, liver, and small intestine were harvested, and the small intestine was gently flushed with saline. After overnight fixation in 10% neutral-buffered formalin, 3-μm paraffin-embedded sections were obtained and stained with H&E (all tissues) or with PAS plus hematoxylin (intestinal samples only). PAS staining reveals complex carbohydrates such as mucinogen, a component of mucus secreted by the goblet cells that are abundant in the intestine.

ApopTag and immunofluorescence staining. The detection of cells undergoing apoptosis was achieved using the ApopTag Red In Situ Apoptosis Detection Kit (Chemicon International). Paraffin-embedded sections were deparaffinized with 3 washes in xylene and serial washes in 100%, 90%, and 70% ethanol, followed by a final wash in distilled water. Cells undergoing apoptosis were detected as specified by the manufacturer, with the modification that samples were incubated overnight at 4°C with working-strength sheep anti-digoxigenin conjugated with rhodamine. For CD3 staining, sections were heat-treated to unmask the antigen, then incubated for 30 minutes with rabbit primary antibody (Biocare Medical) and washed 3 times for 5 minutes. A biotinylated anti-rabbit secondary antibody (Vector Laboratories) was added for 30 minutes, and then slides were washed as described above. Both primary and secondary antibodies were diluted 1:100 with 2% normal goat serum (NGS). Thereafter, sections were incubated for 30 minutes with streptavidin–Alexa 488 conjugate (Invitrogen Corp.) diluted 1:500 in 2% NGS. For the detection of nuclear DNA, sections were incubated for 2 minutes with 300 nmol/l DAPI dilactate solution (Invitrogen Corp.) diluted in PBS, then washed once for 5 minutes with PBS. Sections were observed by fluorescent microscopy (Zeiss Axiovert 200 inverted microscope). Double-channel images were merged using AxioVision software (Zeiss).

Evaluation of mRNA levels using RPA. Organ samples were harvested at the time points indicated in the figure legends and immediately snap-frozen by immersion in liquid nitrogen. Total RNA was isolated from each tissue using TRIzol reagent (Invitrogen Corp.) according to the manufacturer's recommended protocol. RNA was quantified by A_{260} measurements, and 5 μg was hybridized overnight at 56°C to 4.4×10^5 cpm of ^{32}P-labeled antisense RNA probes; the probe templates were kindly provided by Iain Campbell (University of Sydney, Sydney, Australia). As a control for total RNA levels, each template set also contained a probe for an mRNA corresponding to the ribosomal protein L-32. Antisense probes were transcribed in vitro from HindIII linearized DNA templates using T7 RNA polymerase (Promega Corp.) and labeled with ^{32}P-UTP (Amersham Biosciences). After hybridization the samples were treated with RNases A and T1, and then the RNases were inactivated using proteinase K. The samples were then extracted once with phenol chloroform, ethanol-precipitated, washed, dried, resuspended in 5 μl of sample buffer, and subjected to electrophoresis on a 5% acrylamide urea gel run at 2,000 V and 55 W. Autoradiographs were obtained using high-performance autoradiographic film (Amersham Biosciences) at –70°C either overnight or for 3 days. The relative intensities of the bands representing TNF mRNA were determined using the public domain software ImageJ, available from NIH at http://rsb.info.nih.gov/ij/.

Acknowledgments

We are grateful to Annette Lord for excellent secretarial support. This work was supported by NIH grant AI27028. This is manuscript number 17023-NP from the Scripps Research Institute.

Received for publication May 10, 2005, and accepted in revised form November 15, 2005.

Address correspondence to: J. Lindsay Whitton, Department of Neuropharmacology, CVN-9, The Scripps Research Institute, 10550 North Torrey Pines Road, La Jolla, California 92037, USA. Phone: (858) 784-7090; Fax: (858) 784-7380; E-mail: lwhitton@scripps.edu.

1. Whitton, J.L., and Oldstone, M.B.A. 2001. The immune response to viruses. In *Fields virology*. D.M. Knipe and P.M. Howley, editors. Lippincott Williams & Wilkins. Philadelphia, Pennsylvania, USA. 285–320.
2. Kagi, D., et al. 1994. Cytotoxicity mediated by T cells and natural killer cells is greatly impaired in perforin-deficient mice. *Nature.* **369**:31–37.
3. Walsh, C.M., et al. 1994. Immune function in mice lacking the perforin gene. *Proc. Natl. Acad. Sci. U. S. A.* **91**:10854–10858.
4. Slifka, M.K., and Whitton, J.L. 2000. Antigen-specific regulation of T cell-mediated cytokine production. *Immunity.* **12**:451–457.
5. Guidotti, L.G., and Chisari, F.V. 1996. To kill or to cure: options in host defense against viral infection. *Curr. Opin. Immunol.* **8**:478–483.
6. Petersson, K., Forsberg, G., and Walse, B. 2004. Interplay between superantigens and immunoreceptors. *Scand. J. Immunol.* **59**:345–355.
7. Romero, P., Cerottini, J.C., and Speiser, D.E. 2004. Monitoring tumor antigen specific T-cell responses in cancer patients and phase I clinical trials of peptide-based vaccination. *Cancer Immunol. Immunother.* **53**:249–255.
8. Blattman, J.N., et al. 2002. Estimating the precursor frequency of naive antigen-specific CD8 T cells. *J. Exp. Med.* **195**:657–664.
9. Callan, M.F., et al. 1998. Direct visualization of antigen-specific $CD8^+$ T cells during the primary immune response to Epstein-Barr virus In vivo. *J. Exp. Med.* **187**:1395–1402.
10. Yokoyama, M., Zhang, J., and Whitton, J.L. 1995.

DNA immunization confers protection against lethal lymphocytic choriomeningitis virus infection. *J. Virol.* **69**:2684–2688.
11. Whitton, J.L., Yokoyama, M., and Zhang, J. 1996. DNA immunization in an arenavirus model. In *Antiviral immunity*. M. Eibl, C. Huber, H.H. Peter, and U. Wahn, editors. Springer-Verlag. New York, New York, USA. 151–164.
12. Hammarlund, E., et al. 2003. Duration of antiviral immunity after smallpox vaccination. *Nat. Med.* **9**:1131–1137.
13. Tscharke, D.C., et al. 2005. Identification of poxvirus $CD8^+$ T cell determinants to enable rational design and characterization of smallpox vaccines. *J. Exp. Med.* **201**:95–104.
14. Liu, F., Whitton, J.L., and Slifka, M.K. 2004. The rapidity with which virus-specific $CD8^+$ T cells initiate IFNγ synthesis increases markedly over the course of infection, and correlates with immunodominance. *J. Immunol.* **173**:456–462.
15. Slifka, M.K., and Whitton, J.L. 2001. Functional avidity maturation of $CD8^+$ T cells without selection of higher affinity TCR. *Nat. Immunol.* **2**:711–717.
16. Slifka, M.K., and Whitton, J.L. 2000. Activated and memory $CD8^+$ T cells can be distinguished by their cytokine profiles and phenotypic markers. *J. Immunol.* **164**:208–216.
17. Tracey, K.J., and Cerami, A. 1994. Tumor necrosis factor: a pleiotropic cytokine and therapeutic target. *Annu. Rev. Med.* **45**:491–503.
18. Wayte, J., Silva, A.T., Krausz, T., and Cohen, J. 1993. Observations on the role of tumor necrosis factor-alpha in a murine model of shock due to Streptococcus pyogenes. *Crit. Care Med.* **21**:1207–1212.
19. Camenisch, T.D., Koller, B.H., Earp, H.S., and Matsushima, G.K. 1999. A novel receptor tyrosine kinase, Mer, inhibits TNF-α production and lipopolysaccharide-induced endotoxic shock. *J. Immunol.* **162**:3498–3503.
20. Remick, D.G., Kunkel, R.G., Larrick, J.W., and Kunkel, S.L. 1987. Acute in vivo effects of human recombinant tumor necrosis factor. *Lab. Invest.* **56**:583–590.
21. Piguet, P.F., Grau, G.E., Allet, B., and Vassalli, P. 1987. Tumor necrosis factor/cachectin is an effector of skin and gut lesions of the acute phase of graft-vs.-host disease. *J. Exp. Med.* **166**:1280–1289.
22. Piguet, P.F., Vesin, C., Donati, Y., and Barazzone, C. 1999. TNF-induced enterocyte apoptosis and detachment in mice: induction of caspases and prevention by a caspase inhibitor, ZVAD-fmk. *Lab. Invest.* **79**:495–500.
23. Verdugo, P. 1991. Mucin exocytosis [review]. *Am. Rev. Respir. Dis.* **144**:S33–S37.
24. Rothe, J., Mackay, F., Bluethmann, H., Zinkernagel, R., and Lesslauer, W. 1994. Phenotypic analysis of TNFR1-deficient mice and characterization of TNFR1-deficient fibroblasts in vitro. *Circ. Shock.* **44**:51–56.
25. Wong, G.H., Tartaglia, L.A., Lee, M.S., and Goeddel, D.V. 1992. Antiviral activity of tumor necrosis factor is signaled through the 55-kDa type I TNF receptor. *J. Immunol.* **149**:3350–3353.
26. Suresh, M., Singh, A., and Fischer, C. 2005. Role of tumor necrosis factor receptors in regulating CD8 T-cell responses during acute lymphocytic choriomeningitis virus infection. *J. Virol.* **79**:202–213.
27. Bartholdy, C., Christensen, J.P., Wodarz, D., and Thomsen, A.R. 2000. Persistent virus infection despite chronic cytotoxic T-lymphocyte activation in gamma interferon-deficient mice infected with lymphocytic choriomeningitis virus. *J. Virol.* **74**:10304–10311.
28. Whitmire, J.K., Tan, J.T., and Whitton, J.L. 2005. Interferon-γ acts directly on $CD8^+$ T cells to increase their abundance during virus infection. *J. Exp. Med.* **201**:1053–1059.
29. Badovinac, V.P., Corbin, G.A., and Harty, J.T. 2000. Cutting edge: OFF cycling of TNF production by antigen-specific $CD8^+$ T cells is antigen independent. *J. Immunol.* **165**:5387–5391.
30. Slifka, M.K., Rodriguez, F., and Whitton, J.L. 1999. Rapid on/off cycling of cytokine production by virus-specific $CD8^+$ T cells. *Nature.* **401**:76–79.
31. Gaur, U., and Aggarwal, B.B. 2003. Regulation of proliferation, survival and apoptosis by members of the TNF superfamily. *Biochem. Pharmacol.* **66**:1403–1408.
32. Springer, T., Galfre, G., Secher, D.S., and Milstein, C. 1979. Mac-1: a macrophage differentiation antigen identified by monoclonal antibody. *Eur. J. Immunol.* **9**:301–306.
33. McFarland, H.I., Nahill, S.R., Maciaszek, J.W., and Welsh, R.M. 1992. CD11b (Mac-1): a marker for $CD8^+$ cytotoxic T cell activation and memory in virus infection. *J. Immunol.* **149**:1326–1333.
34. Hamann, D., et al. 1997. Phenotypic and functional separation of memory and effector human $CD8^+$ T cells. *J. Exp. Med.* **186**:1407–1418.
35. Black, R.A., et al. 1997. A metalloproteinase disintegrin that releases tumour-necrosis factor-α from cells. *Nature.* **385**:729–733.
36. Monastra, G., et al. 1996. Membrane form of TNFα induces both cell lysis and apoptosis in susceptible target cells. *Cell Immunol.* **171**:102–110.
37. Kontoyiannis, D., et al. 2002. Genetic dissection of the cellular pathways and signaling mechanisms in modeled tumor necrosis factor-induced Crohn's-like inflammatory bowel disease. *J. Exp. Med.* **196**:1563–1574.
38. Kontoyiannis, D., et al. 2001. Interleukin-10 targets p38 MAPK to modulate ARE-dependent TNF mRNA translation and limit intestinal pathology. *EMBO J.* **20**:3760–3770.
39. Papadakis, K.A., and Targan, S.R. 2000. Role of cytokines in the pathogenesis of inflammatory bowel disease. *Annu. Rev. Med.* **51**:289–298.
40. Ruuls, S.R., et al. 2001. Membrane-bound TNF supports secondary lymphoid organ structure but is subservient to secreted TNF in driving autoimmune inflammation. *Immunity.* **15**:533–543.
41. Piguet, P.F., Vesin, C., Guo, J., Donati, Y., and Barazzone, C. 1998. TNF-induced enterocyte apoptosis in mice is mediated by the TNF receptor 1 and does not require p53. *Eur. J. Immunol.* **28**:3499–3505.
42. Varfolomeev, E.E., et al. 1998. Targeted disruption of the mouse Caspase 8 gene ablates cell death induction by the TNF receptors, Fas/Apo1, and DR3 and is lethal prenatally. *Immunity.* **9**:267–276.
43. Leon, L.R. 2004. Hypothermia in systemic inflammation: role of cytokines. *Front. Biosci.* **9**:1877–1888.
44. Conti, B., Tabarean, I., Andrei, C., and Bartfai, T. 2004. Cytokines and fever. *Front. Biosci.* **9**:1433–1449.
45. Leon, L.R., White, A.A., and Kluger, M.J. 1998. Role of IL-6 and TNF in thermoregulation and survival during sepsis in mice. *Am. J. Physiol.* **275**:R269–R277.
46. Boulant, J.A. 2000. Role of the preoptic-anterior hypothalamus in thermoregulation and fever. *Clin. Infect. Dis.* **31**(Suppl. 5):S157–S161.
47. Rizk, N.M., Joost, H.G., and Eckel, J. 2001. Increased hypothalamic expression of the p75 tumor necrosis factor receptor in New Zealand obese mice. *Horm. Metab. Res.* **33**:520–524.
48. Shibata, M., and Blatteis, C.M. 1991. Differential effects of cytokines on thermosensitive neurons in guinea pig preoptic area slices. *Am. J. Physiol.* **261**:R1096–R1103.
49. Shibata, M., and Blatteis, C.M. 1991. Human recombinant tumor necrosis factor and interferon affect the activity of neurons in the organum vasculosum laminae terminalis. *Brain Res.* **562**:323–326.
50. Verdugo, P., Deyrup-Olsen, D., Aitken, M., Villalon, M., and Johnson, D. 1987. Molecular mechanism of mucin secretion. I. The role of intragranular charge shielding. *J. Dent. Res.* **66**:506–508.
51. Nguyen, T., Chin, W.C., and Verdugo, P. 1998. Role of Ca^{2+}/K+ ion exchange in intracellular storage and release of Ca2+. *Nature.* **395**:908–912.
52. Pollock, J., et al. 2002. TNF-α receptors simultaneously activate Ca^{2+} mobilisation and stress kinases in cultured sensory neurones. *Neuropharmacology.* **42**:93–106.
53. Koike, K., et al. 1991. Tumor necrosis factor-alpha stimulates prolactin release from anterior pituitary cells: a possible involvement of intracellular calcium mobilization. *Endocrinology.* **128**:2785–2790.
54. Rizzuto, R., et al. 2003. Calcium and apoptosis: facts and hypotheses. *Oncogene.* **22**:8619–8627.
55. Aichele, P., et al. 1997. Peptide antigen treatment of naïve and virus-immune mice: antigen-specific tolerance versus immunopathology. *Immunity.* **6**:519–529.
56. Hoebe, K., Janssen, E., and Beutler, B. 2004. The interface between innate and adaptive immunity. *Nat. Immunol.* **5**:971–974.
57. Satoh, M., Oshima, H., Abe, S., Yamazaki, M., and Mizuno, D. 1987. Role of in vivo scavenger function of macrophages in priming for endogenous production of tumor necrosis factor. *J. Biol. Response Mod.* **6**:499–511.
58. Bilsborough, J., et al. 2002. TNF-mediated toxicity after massive induction of specific $CD8^+$ T cells following immunization of mice with a tumor-specific peptide. *J. Immunol.* **169**:3053–3060.
59. Remick, D.G., and Kunkel, S.L. 1993. Pathophysiologic alterations induced by tumor necrosis factor. *Int. Rev. Exp. Pathol.* **34**:7–25.
60. Kort, W.J., et al. 1998. A microchip implant system as a method to determine body temperature of terminally ill rats and mice. *Lab. Anim.* **32**:260–269.